

Inclusion Complexes of β -Cyclodextrin with Keto/Enol Tautomers of 2-Acetyl-1-tetralone. A Comparative Study

EMILIA IGLESIAS

Departamento de Química Física e E. Q. I, Facultad de Ciencias, Universidad de La Coruña, 15071-La Coruña, Spain
E-mail: *qfemila@udc.es*

(Received: 21 June 2004; in final form: 27 September 2004)

Key words: 2-acetyl-cyclopentanone, 2-acetyl-1-tetralone, β -cyclodextrin, enol-nitrosation, inclusion complexes, tautomerization

Abstract

The keto–enol interconversion of 2-acetyl-1-tetralone (ATLO) and of 2-acetyl-cyclohexanone (ACHE) occurs at measurable rates in aqueous acid or neutral medium. This finding allowed us to determine the keto–enol equilibrium constants, K_E , by following two distinct methods. Both methodologies afford results in complete agreement. The first one is a test of the Beer-Lambert law under two different experimental conditions that contain the substrate only in the enol form or in a mixture of both tautomers in equilibrium. The second method analyses the UV-absorption spectrum of each substrate under keto–enol equilibrium in aqueous β -cyclodextrin (β -CD) solutions of variable concentration: the presence of β -CD increases the percentage of the enol due to the formation of 1:1 inclusion complexes between this tautomer and β -CD. Rates of keto–enol tautomerization, in neutral and acid medium, and of nitrosation in acid medium under non equilibrium conditions have also been measured. Throughout the study, the presentation of the results is done by comparing the different behaviour observed between ATLO and ACHE. While the enol of ACHE included into the β -CD cavity shows to be unreactive either in tautomerization or in nitrosation, in the case of ATLO it is observed tautomerization through the complexed enol. In addition, with ACHE only the enol tautomer forms inclusion complexes with β -CD, whereas with ATLO the keto tautomer enters also to the β -CD cavity, however the stability constant with the enol is near 3-fold that of the keto isomer. These main differences can be rationalized on the basis of the molecular structure of these diketones.

Introduction

1,3-Diketones, such as 2-acetyl-1-tetralone (ATLO) or 2-acetyl-cyclohexanone (ACHE) have one ionisable proton and three possible tautomeric forms (keto, enol, and enolate), whose equilibrium ratios may be severely affected by changes in the media in which they are dissolved. The keto (KH) and enol (EH) forms are both present in aqueous acid or neutral solutions in measurable proportions. But the enol amount increases in apolar and/or aprotic (non-hydrogen bond donor or acceptor) solvents, being in some cases the predominant species. In aqueous alkaline medium, the enolate is rapidly generated, which in some situations is the only existing species [1].

The formulation of many reaction mechanisms can be aided by data on the effect of solvents on the rates of the reaction [2, 3]. For a given solvent, or any homogeneous solution, the dielectric constant is an important parameter; however, its properties are due to a combination of many interactions including dipole–dipole, charge–dipole, charge–charge, hydrogen bonding, etc

[4, 5]. For a micro-heterogeneous solution, such as aqueous surfactant or cyclodextrin solutions, hydrophobic interactions play also a decisive role [6–10].

There have been a large number of studies into the tautomeric equilibria in general [11–13] and of 1,3-dicarbonyl compounds in particular [14, 15] using a great variety of techniques, and carrying out in water, in organic solvents, and recently in aqueous solutions of surfactants forming micelles [16] and of cyclodextrins [17]. We have measured the keto–enol tautomerization constants [18] and the keto–enol equilibrium constants of several 1,3-dicarbonyl compounds in microheterogeneous media by UV–vis spectroscopy and potentiometry [19]. The electronic spectroscopy appears to us as the most reliable method for these compounds because it only requires low concentrations of the substance to afford large changes of the optical density of the solution, thus conducting to accurate data on avoiding the use of drastic experimental conditions.

In this paper, we provide a comparative and systematic study of the keto–enol tautomerization of ATLO and ACHE in water in the absence and presence of

β -cyclodextrin. Different methods and experimental conditions have been used to design two distinct forms to measure the keto–enol equilibrium constants, K_E , as well as the tautomeric microscopic constants, with excellent agreement between them.

Experimental

2-Acetyl-1-tetralone (Aldrich) was used without any additional purification. Dioxane (spectrophotometric grade) was dried with molecular sieves. All other reagents (Aldrich or Merck) were used as received. Stock solutions of ATLO were prepared in dried dioxane. Aqueous solutions of the rest of reagents were prepared with double distilled water obtained from a permanganate solution.

UV–vis absorption spectra and kinetic measurements were recorded with a double-beam spectrophotometer (Uvikon 942 or XL) provided with a thermostatted cell holder. A matched pair of quartz cells with $l = 1$ cm light was used. Kinetic measurements were carried out under pseudo-first order conditions, with the concentration of ATLO, the limiting reagent, being more than 20 times lower than that of the others reactants. Both the enol tautomerization and enol nitrosation reactions have been studied by monitoring the decreasing absorbance at $\lambda = 343$ or 291 nm due to the enol form, respectively of ATLO or ACHE. Both reactions were initiated by injecting 10–40 μL of a stock dioxane solution of diketone into 3.0 mL of water containing the rest of the reagents. The experimental data (absorbance–time, A - t) were fitted to the pseudo-first order integrated equation, Equation (1), by obtaining satisfactory correlation coefficients ($r > 0.9999$) and residuals in every experiment.

$$A = A_\infty + (A_0 - A_\infty)e^{-k_0 t} \quad (1)$$

The observed rate constant, k_0 , of tautomerization is the sum of the rate constants corresponding to enol–ketonization, k_0^k , and keto–enolization, k_0^e ($k_0 = k_0^k + k_0^e$).

Molecular dimensions were estimated by Hypercube Hyper Chem 7.0 on personal computer.

Results and discussion

A diluted solution ($\sim 8 \times 10^{-5}$ M) of ATLO, either in water or organic solvents, shows two absorption bands whose relative intensities change with both the time and the solvent (Figure 1). These two bands, with maxima at 343 nm and 254 nm, were tentatively assigned to the enol (EH) and keto (KH) forms, respectively: the only two tautomeric forms in equilibrium, an assumption that is confirmed by the presence of clearly defined isosbestic points in this region (at 274 and 238 nm).

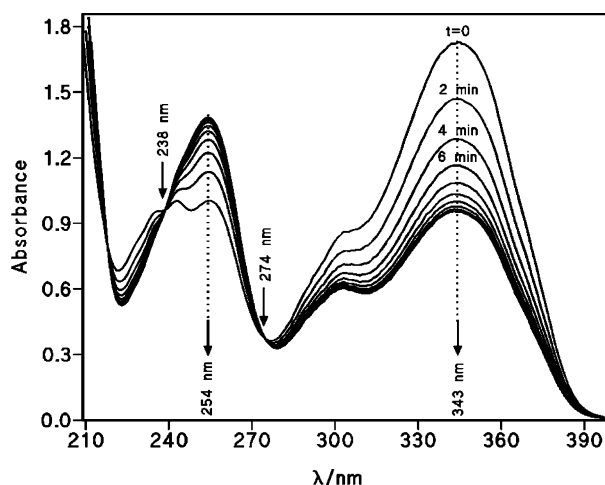


Figure 1. Absorption spectra of ATLO (8×10^{-5} M) in water taken every 2 min showing the absorbance decrease at 343 nm due to enol–ketonization.

Nevertheless, the absorbance at 343 nm decreases with time when ATLO dissolved in dioxane is diluted in water (10 μL in 3.0 mL); whereas the contrary is observed if a concentrated aqueous ATLO solution is diluted in e.g., dioxane – or DMSO – (100 μL in 2.9 mL). The reaction being observed is the slow keto–enol tautomerization, i.e., ATLO is fully enolized in aprotic solvents such as dioxane or DMSO, while a mixture of the two tautomers (keto and enol) is present in water, and their interconversion is slow, as we have already found with 2-acetyl-cyclohexanone [18] but in contrast to that observed with 2-acetyl-cyclopentanone [19b] or even with other 1,3-diketones [16]. Therefore, Figure 1 shows the reaction spectra of enol–ketonization as the neat reaction, but the process corresponds to the keto–enol equilibrium approach.

We make use of these experimental features to measure keto–enol equilibrium constants in water by following different methodologies.

1. *Beer–Lambert law.* Rate constants for enol–ketonization were determined in water at 25 °C for different initial ATLO concentrations. The results reported in Table 1 show that the extrapolated values of the initial absorbance ($t \rightarrow 0$), A_0 , at $\lambda = 343$ nm increase proportional to [ATLO]; the same trend is observed with A_∞ values, i.e., the optimised absorbance readings at $t \rightarrow \infty$. At the beginning of the tautomerization reaction, the practical totality of ATLO is in the enol form, then Equation (2) can be used to relate A_0 and [ATLO]; whereas at the end of the reaction, a mixture of both keto and enol tautomers exists in equilibrium, being K_E the corresponding equilibrium constant: $\text{KH} \rightleftharpoons \text{EH}$, K_E ; then, Equation (3) can be obtained to explain the variation of A_∞ as a function of [ATLO]. Therefore, K_E can be determined as the quotient of $A_\infty/(A_0 - A_\infty)$ at each [ATLO]. The resulting data, shown also in Table 1 (entry four), give $K_E = 0.95$.

Table 1. Initial (A_o) and final (A_∞) absorbance readings at $\lambda = 343$ nm obtained in the kinetic study of ATLO tautomerization in water by fitting the experimental data (A_t) to Equation (1), along with the observed k_o values as a function of ATLO concentration

[ATLO]/M	A_o ($\lambda = 343$ nm)	A_∞ ($\lambda = 343$ nm)	$k_o/$ 10^{-3} s^{-1}	K_E
1.60	0.285	0.150	3.66	1.11
2.40	0.403	0.206	3.65	1.05
3.20	0.540	0.263	3.65	0.95
4.80	0.814	0.391	3.64	0.92
6.40	1.050	0.481	3.62	0.85
8.0	1.348	0.638	3.61	0.90
9.6	1.567	0.747	3.60	0.91
11.2	1.802	0.882	3.63	0.96
Average:			3.62	0.95

$$A_{343}^o = \epsilon_{\text{EH}} l [\text{ATLO}] \quad (2)$$

$$A_{343}^\infty = \epsilon_{\text{EH}} l \frac{K_E}{1 + K_E} [\text{ATLO}] \quad (3)$$

Alternatively, K_E can be obtained from the ratio of the slopes of the linear plots of A_o against [ATLO] (Equation 2) and of A_∞ against [ATLO] (Equation 3). The resulting slopes were $16,300 \pm 150 \text{ M}^{-1} \text{ cm}^{-1}$ ($cc = 0.999_7$) for the former plot, and $7700 \pm 125 \text{ M}^{-1} \text{ cm}^{-1}$ ($cc = 0.999_2$) for the latter. The first value corresponds to the molar absorption coefficient of the enol of ATLO, ϵ_{EH} , and the combination of both figures yields $K_E = 0.90$ in good agreement with the previous value.

2. *Keto-enol equilibrium in the presence of β -CD.* At constant [ATLO] ($6.4 \times 10^{-5} \text{ M}$), we analysed the effect of $[\text{H}^+]$ (added as HCl). The results are listed in Table 2, along with the calculated values of K_E obtained from the absorbance readings at each $[\text{H}^+]$. It can be noted a moderate catalysis on increasing the acidity of the reaction medium, Equation (4), by observing good straight lines in the plot of k_o against $[\text{H}^+]$, with $k_w = (3.55 \pm 0.07) \times 10^{-3} \text{ s}^{-1}$ and $k_H = (1.08 \pm 0.01) \times 10^{-2} \text{ M}^{-1} \text{ s}^{-1}$ ($cc = 0.999_7$).

$$k_o = k_w + k_H [\text{H}^+] \quad (4)$$

Table 2. Optimized values of A_o , A_∞ , and k_o in the fitting process of the experimental data A_t to Equation (1) for the kinetic study of ATLO ([ATLO] = $6.4 \times 10^{-5} \text{ M}$) tautomerization at different $[\text{H}^+]$

$[\text{H}^+]/\text{M}$	$k_o/10^{-3} \text{ s}^{-1}$	A_o ($\lambda = 343$ nm)	A_∞ ($\lambda = 343$ nm)	K_E
0.017	3.74	1.089	0.521	0.92
0.033	3.89	1.139	0.546	0.92
0.050	4.09	1.119	0.534	0.915
0.067	4.27	1.134	0.543	0.92
0.083	4.46	1.147	0.550	0.92
0.10	4.64	1.152	0.551	0.92
0.12	4.81	1.144	0.549	0.92
Average:				0.92

Tautomerization rates of ACHE are slower than that observed for ATLO; for example, with ACHE the influence of the acidity gives: $k_w = (1.39 \pm 0.01) \times 10^{-3} \text{ s}^{-1}$ and $k_H = (6.09 \pm 0.06) \times 10^{-3} \text{ M}^{-1} \text{ s}^{-1}$.

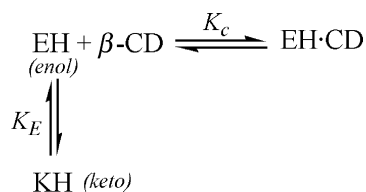
Subsequently, we studied the influence of β -cyclodextrin (β -CD) on enol-ketonization of ATLO in water and in aqueous hydrochloric acid (0.050 M). To start the reaction, a small volume ($= 10 \mu\text{L}$ when the reaction was carried in water, and $40 \mu\text{L}$, in aqueous HCl) of a stock dioxane solution of ATLO was added to the reaction sample containing the rest of the reagents ($V_t = 3.0 \text{ mL}$). Either in neutral or in acid media, the absorbance readings at infinite time (A_∞) increase with β -CD concentration (the ATLO concentration is kept constant). This finding can be explained by proposing the formation of inclusion complexes between the enol (EH) and β -CD, which increases the total enol concentration. Therefore it can be calculated the values of K_E^{ap} at each $[\beta\text{-CD}]$ by application of Equation (5), in which both quantities, A_o and $A_o - A_\infty$, were obtained experimentally.

$$K_E^{\text{ap}} = \frac{[\text{EH}]_t}{[\text{KH}]} = \frac{A_\infty}{A_o - A_\infty} \quad (5)$$

The variation of K_E^{ap} as a function of $[\beta\text{-CD}]$ is reported in Figure 2(a). For comparative purposes, Figure 2(b) shows the corresponding results obtained with ACHE. Whereas in the latter case K_E^{ap} increases proportional to $[\beta\text{-CD}]$, with ATLO the same plot describes saturation curves. One may also note that, for the same $[\beta\text{-CD}]$, K_E^{ap} reach higher values when the volume of the stock dioxane diketone solution is small ($10 \mu\text{L}$ against $40 \mu\text{L}$). On the other hand, the neat observed effect is higher with ATLO than with ACHE, which can be attributed to a more effective interaction between the enol of ATLO and the β -CD cavity than between the latter and the enol of ACHE, a less hydrophobic species.

The behaviour observed with ACHE have been explained through the formation of 1:1 inclusion complexes between the enol and β -CD, Scheme 1, from which it can be derived the Equation (6) that predicts a linear increase of K_E^{ap} with $[\beta\text{-CD}]$ as it is experimentally found.

The least-squares adjustment of this equation to the experimental points of K_E^{ap} - $[\beta\text{-CD}]$, affords the values of the adjustable parameters, K_E and K_c^{ap} , depicted in Table 3.



Scheme 1. Possible equilibria involved in aqueous β -CD solutions of ACHE.

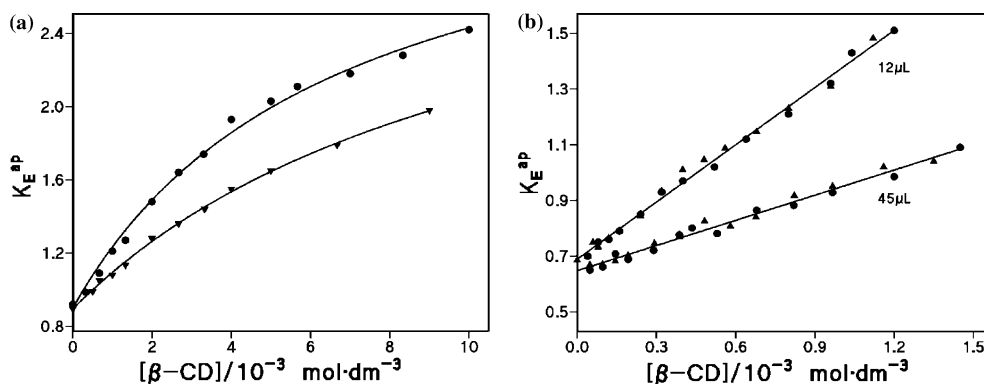


Figure 2. Variation of K_E^{ap} as a function of $[\beta\text{-CD}]$ for the case of (a) 2-acetyl-1-tetralone in (●) water, 10 μL of the stock dioxane ATLO solution, and (▼) aqueous hydrochloric acid 0.050 M, 40 μL of the stock dioxane ATLO solution; and for (b) 2-acetyl-cyclohexanone in (●) water and (▲) aqueous hydrochloric acid 0.033 M.

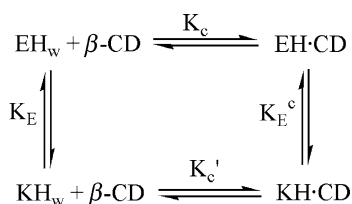
Table 3. Equilibrium constants determined in the study of the effect of $\beta\text{-CD}$ on the keto–enol equilibrium of both ATLO and ACHE in aqueous acid or neutral solutions containing small amounts of dioxane. See Schemes 1 and 2 for the meaning of the equilibrium constants

[dioxane]/M	K_E	K_c^{ap}/M^{-1}	$K_c'^{ap}/M^{-1}$	K_c/M^{-1}	K_c'/M^{-1}
<i>2-acetyl-1-tetralone (ATLO)</i>					
0.040	0.89 ± 0.02	609 ± 30	158 ± 10	$K_I = 13.0 M^{-1}$	240
0.15	0.91 ± 0.01	310 ± 20	82 ± 9	917	242
<i>2-acetyl-cyclohexanone (ACHE)</i>					
0.047	0.69 ± 0.01	95.5 ± 2.0	–	177	–
0.17	0.65 ± 0.03	46 ± 1	–	175	–

$$K_E^{ap} = \frac{[\text{EH}]_w + [\text{EH} \cdot \text{CD}]}{[\text{KH}]_w} = K_E(1 + K_c^{ap}[\beta\text{-CD}]) \quad (6)$$

To interpret the data in Figure 2(a) obtained in the case of ATLO it is necessary to consider that the keto tautomer forms also inclusion complexes with $\beta\text{-CD}$. Therefore, once the keto–enol equilibrium is reached ($t \rightarrow \infty$), the involved equilibria are those displayed in Scheme 2, from which it is derived the Equation (7) that relates K_E^{ap} with $[\beta\text{-CD}]$. The curves of Figure 2(a) were drawn using a non-linear regression analysis of the experimental points, $K_E^{ap}-[\beta\text{-CD}]$, by means of Equation (7). The values of optimised parameters K_E , K_c^{ap} and $K_c'^{ap}$ are also listed in Table 3.

$$K_E^{ap} = \frac{[\text{EH}]_t}{[\text{KH}]_t} = \frac{[\text{EH}]_w + [\text{EH} \cdot \text{CD}]}{[\text{KH}]_w + [\text{KH} \cdot \text{CD}]} = \frac{K_E(1 + K_c^{ap}[\beta\text{-CD}])}{1 + K_c'^{ap}[\beta\text{-CD}]} \quad (7)$$



Scheme 2. Postulated equilibrium steps that occur in aqueous $\beta\text{-CD}$ solutions of ATLO.

As it can be seen, K_E values are independent of dioxane concentration. This equilibrium constant achieved in water increases with the dioxane percentage, i.e., when the dielectric constant of water–dioxane mixtures decreases. According to Anderson [20], the relative permittivity of water–dioxane mixtures can be determined as: $\epsilon_s = 78.5 - 12.6w - 50.5w^2 + 48.5w^3$, where w is the weight fraction dioxane. Then, under our experimental conditions the maximum variation of ϵ_s should be from 78.25 to 77.4, that is, practical the same of pure water, a fact which explain the constancy in K_E . For the same reason, K_c^{ap} and $K_c'^{ap}$ should not be different on varying the dioxane concentration from 0.04 to 0.17 M, unless the dioxane molecules compete with the enol/keto molecules for the cyclodextrin cavity. Obviously, either ATLO or ACHE are more hydrophobic than the dioxane molecules (miscible with water); nevertheless, the concentration of dioxane are much higher than those of ATLO of ACHE, a fact for the logical consideration of the competition between dioxane and substrate molecules for the cyclodextrin cavity. Therefore, if one introduces the process: $\text{Diox} + \beta\text{-CD} \rightleftharpoons \text{Diox} \cdot \text{CD}$, K_I , in both Schemes 1 and 2, and taking into account now that $[\beta\text{-CD}]_o = [\beta\text{-CD}] + [\text{Diox} \cdot \text{CD}]$, the apparent inclusion equilibrium constant, K_c^{ap} or $K_c'^{ap}$, given in Table 3 are related to the true equilibrium constants (K_c and K_c') by the expressions of Equation (8).

$$K_c^{\text{ap}} = \frac{K_c}{1 + K_1[\text{Diox}]} \quad \text{and} \quad K_c'^{\text{ap}} = \frac{K_c'}{1 + K_1[\text{Diox}]} \quad (8)$$

From our results given in Table 3, we determine a mean value of $K_1 = 15 \text{ M}^{-1}$. Unfortunately, we have not found any literature reference to this result; nevertheless, the stability constant between dioxane molecules and α -CD is 4.5 M^{-1} [21] and a higher value should be expected for the inclusion with β -CD, in addition, a value of 15 M^{-1} is in good agreement with that reported for similar substrates [22]. On the other hand, this value affords the values of K_c and K_c' listed in Table 3. In the case of ACHE, it was not detected the complexation of the keto form, whereas both tautomers of ATLO form inclusion complexes, like we have already been observed with benzoylacetone [17a], a substrate that possesses a phenyl ring like ATLO.

The results obtained in the following section on the kinetic study of the effect of β -CD on rates of either tautomerization or nitrosation support the preceding treatment.

3. *β -Cyclodextrin affects rates of tautomerization and nitrosation.* We analyse here the influence of β -CD upon

the tautomerization reaction performed in both water and aqueous hydrochloric acid (0.050 M). To start the reaction, an aliquot of 10 or 40 μL of a stock dioxane ATLO solution was diluted into 3.0 mL of water or of aqueous hydrochloric acid, respectively. The decrease in absorbance at 343 nm was recorded as a function of time to obtain the pseudo-first order rate constant, k_o . The k_o versus $[\beta\text{-CD}]$ profiles can be shown in Figure 3, along with the similar plot obtained with ACHE.

Rates of enol ketonization are retarded by the addition of β -CD and catalysed by H^+ . The effect is stronger for ATLO than for ACHE and decreases with the high percentage of dioxane in the reaction mixture. On the other hand, Figure 4 shows the different behaviour found for the reciprocal plot of k_o against $[\beta\text{-CD}]$ with both substrates: while good straight lines are drawn with ACHE, saturation curves are obtained with ATLO either if the reaction is performed in neutral or aqueous acid medium.

The behaviour found for ACHE can be explained on the basis of the formation of 1:1 inclusion complexes between the enol of ACHE and β -CD: the enol must protrude deeper inside the β -CD cavity, in a way that the encapsulated enol is protected from the water

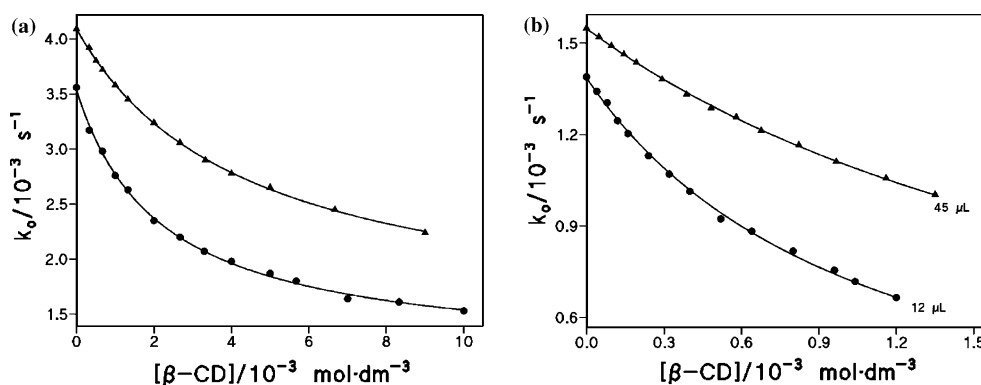


Figure 3. Influence of β -CD on the observed rate constant, k_o , for the tautomerization of (a) 2-acetyl-1-tetralone in (●) water 10 μL of dioxane – and in (▲) aqueous hydrochloric acid 0.050 M of 40 μL of dioxane –, and of (b) 2-acetyl-cyclohexanone in (●) water 12 μL of dioxane – and in (▲) aqueous hydrochloric acid 0.033 M 45 μL of dioxane.

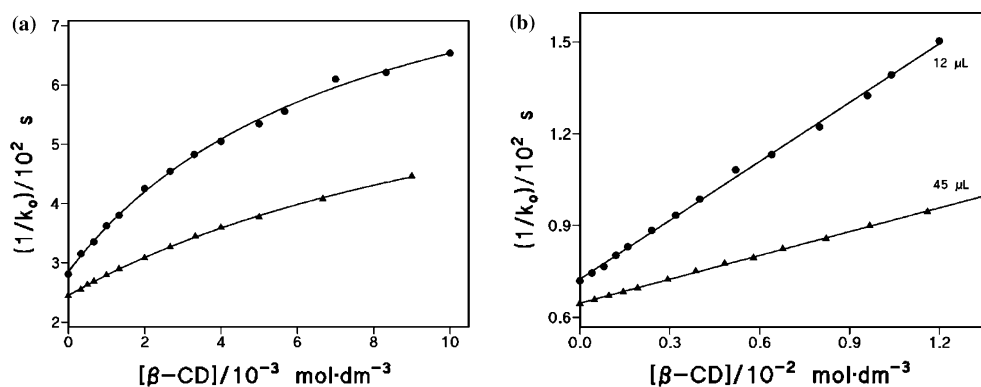


Figure 4. Reciprocal plot of k_o against $[\beta\text{-CD}]$ obtained in the tautomerization of (a) 2-acetyl-1-tetralone and (b) 2-acetyl-cyclohexanone. The symbols are the same as in Figure 3.

molecules or H_3O^+ , necessary to carry on the tautomerization. Therefore, by considering the formation of non reactive inclusion complexes, the observed rate constant, k_o , fits Equation (9) that agrees with the observed inhibition effect and also with the straight lines drawn in the plots of $1/k_o$ against $[\beta\text{-CD}]$, Figure 4. The results of K_o^w , K_c^{ap} , and K_c , listed in Table 4, are in good concordance with with data in Table 3 that have been obtained under equilibrium conditions.

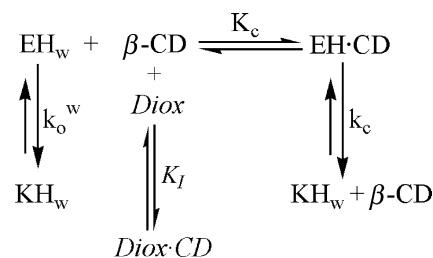
$$k_o = \frac{k_o^w}{1 + K_c^{\text{ap}}[\beta - \text{CD}]} \quad (9)$$

The experimental facts observed for the case of ATLO, shown in Figures 3(a) and 4(a), can be rationalized by proposing the formation of reactive 1:1 inclusion complexes between the enol of ATLO and β -CD. The operating reaction mechanism is that of Scheme 3 from which Equation (10) may be obtained. Like in these experiments, the total initial concentration is in the enol form, the K_c^{ap} corresponds to the stability constants of the complexes formed between the enol and β -CD in the presence of the amount of dioxane indicated in the legend of the figures and also in Table 4. The lines shown in the figures correspond to the fit of Equation (10) to the experimental points when the values of the adjustable parameters k_o^w , k_c and K_c^{ap} are those reported in Table 4.

It can be seen the good agreement between K_c values determined here and the same values obtained under equilibrium conditions (see Table 3). In addition, the reactivity of the free enol is almost 3-fold higher than that included inside the β -CD. This finding is indicative of the lower polarity of the β -CD cavity either due to the lower (or null) water content or the strong decrease of the acid–basic properties of the water molecules inside the cavity.

$$k_o = \frac{k_o^w + k_c K_c^{\text{ap}}[\beta - \text{CD}]}{1 + K_c^{\text{ap}}[\beta - \text{CD}]} \quad (10)$$

As expected, the experimental points fit quite well Equation (10) derived from Scheme 3 that does not



Scheme 3. Reaction mechanism of ATLO tautomerization in aqueous β -CD solutions.

consider the inclusion of keto tautomer. The reason for this treatment is the new experimental situation; here we start with all initial ATLO concentration in the enol (EH) form, thus the only established equilibrium since the beginning of the reaction is K_c ; in fact, the obtained values of K_c are in good concordance with those of Table 3, determined under keto–enol equilibration. The results obtained in studying the nitrosation reaction further corroborates this assumption.

The nitrosation is a typical reaction of enols and faster than the tautomerization reaction. On the other hand, the enol is the only tautomer reactive in nitrosation. In other words, this reaction only detects the enol. The nitrosation of both substances, ATLO and ACHE, was studied in aqueous hydrochloric acid with $[\text{nitrite}] = 1.7 \times 10^{-3} \text{ M}$ in high excess over the total concentration of diketone ($\sim 10^{-5} \text{ M}$). As it can be seen in Figure 5 for the case of ATLO, the rate of the reaction is reduced by the presence of β -CD. For both substrates, the reciprocal plot of k_o increases proportional to $[\beta\text{-CD}]$, describing good straight lines (Figure 5(b)). These observations point to a rapid establishment of the equilibrium between free and complexed enol with β -CD (of stoichiometry 1:1) and the low nitrosation path through only the enol existing in the bulk water phase.

In aqueous hydrochloric solutions of sodium nitrite, the nitrosation may be promoted either by NO^+ or by ClNO , whose reagents exist in water at very low concentrations, because they are generated in

Table 4. Rate and equilibrium constants obtained in the kinetic study of the keto–enol tautomerization reaction and of enol nitrosation reaction in water

Substrate	Reaction	Vol. dioxane	Medium	$k_o^w/10^{-3}\text{s}^{-1}$	$k_c/10^{-3}\text{s}^{-1}$	$K_c^{\text{ap}}/\text{M}^{-1}$	K_c/M^{-1}
ACHE	Tautomerization	12 μL	water	1.393 ± 0.008	–	90 ± 2	153
ACHE	Tautomerization	12 μL	0.033 M ^(a)	1.58	–	94 ± 1	160
ACHE	Tautomerization	12 μL	0.066 M ^(a)	1.77 ± 0.06	–	95.8 ± 1.5	163
ACHE	Tautomerization	45 μL	water	1.392 ± 0.003	–	41.6 ± 0.5	153
ACHE	Tautomerization	45 μL	0.033 M ^(a)	1.548 ± 0.002	–	40.4 ± 0.3	148
ACHE	Tautomerization	45 μL	0.066 M ^(a)	1.705 ± 0.004	–	40.0 ± 0.7	147
ACHE	Nitrosation	12 μL	0.033M ^(a)	7.78 ± 0.03	–	117 ± 2	205
ATLO	Tautomerization	10 μL	water	3.68 ± 0.02	1.21	538 ± 20	861
ATLO	Tautomerization	40 μL	0.05 M ^(a)	4.12 ± 0.01	1.35	272 ± 7	884
ATLO	Nitrosation	40 μL	0.017 M ^(a)	6.05 ± 0.05	–	280 ± 10	910

^(a)Aqueous hydrochloric acid at the indicated concentration.

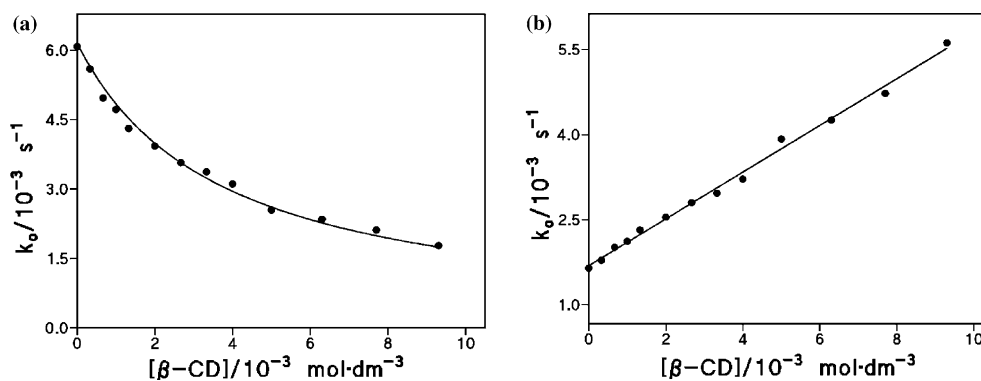
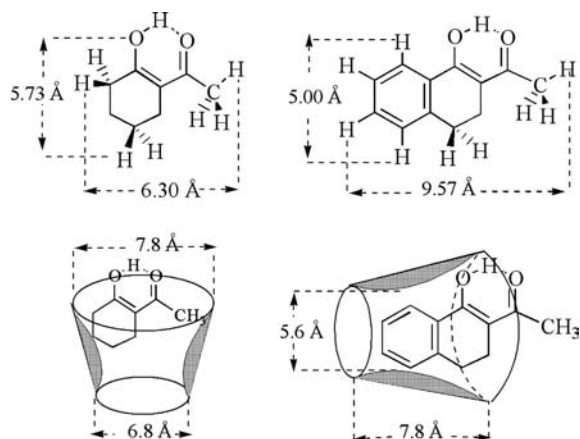


Figure 5. (a) Variation of k_o as a function of $[\beta\text{-CD}]$ for the nitrosation of the enol of 2-acetyl-1-tetralone at $[\text{nitrite}] = 1.7 \times 10^{-3} \text{ M}$, $[\text{H}^+] = 0.015 \text{ M}$ and (b) reciprocal plot of k_o against $[\beta\text{-CD}]$.

the processes: $\text{HNO}_2 + \text{H}^+ \rightleftharpoons \text{NO}^+ \cdot \text{OH}_2$, $K_{\text{NO}} = 3 \times 10^{-7} \text{ M}^{-1}$ or $\text{HNO}_2 + \text{H}^+ + \text{Cl}^- \rightleftharpoons \text{ClNO} + \text{H}_2\text{O}$, $K_{\text{ClNO}} = 1.14 \times 10^{-3} \text{ M}^{-2}$. Therefore, the probability of the existence of significant amounts of NO^+ or ClNO (highly hydrophilic species) inside the $\beta\text{-CD}$ cavity, necessary to occur the reaction *via* the complexed enol, is very small. In fact, an inspection of the data shown in Figures 3(a) and 5(a) reveals the lower inhibition factor (< 2) observed in tautomerization than that in nitrosation (> 3), because in the latter reaction, $\beta\text{-CD}$ protect completely the included enol but not in the former.

Solid lines in Figure 5 were obtained in the fit of Equation (9) to the experimental points, with the values of k_o^w and K_c^{ap} reported in Table 4. It can be noted the much higher rates observed in nitrosation than in tautomerization and also the good agreement between K_c values obtained here and those determined either from tautomerization studies or under equilibrium conditions (Table 3).

Finally, the different behaviour observed between ACHE and ATLO for the effect of $\beta\text{-CD}$ in tautomerization rates, can be understood by considering the possible conformations of the enol-inclusion complexes given in Scheme 4. Taking into account the dimensions



Scheme 4. Proposed conformations of enol $\beta\text{-CD}$ inclusion complexes.

of the $\beta\text{-CD}$ host and the enol guest of both ACHE and ATLO of the optimised structures for the gas phase, the conformation adopted for the inclusion complex may be different in each case. The large size of the enol of ATLO forces the lengthwise inclusion as the only possible manner to do it which leaves an important part of the molecule outside the cavity, whereas the enol of ACHE can protrude the $\beta\text{-CD}$ cavity in a different way that protects totally the reactive site from the attack of even the solvent molecules.

Conclusions

The main observation that deserves to remark is that the similarity of molecular structures between substrates does not always guarantee the same behaviour. Both 2-acetyl-cyclohexanone and 2-acetyl-1-tetralone undergo slow tautomerization in aqueous acid or neutral medium. The presence of $\beta\text{-cyclodextrin}$ reduces the rates of either tautomerization or nitrosation due to the formation of 1:1 inclusion complexes between the enol and $\beta\text{-CD}$, which are much more stable with the enol of ATLO than with that of ACHE. In the same sense, the reactivity of ATLO is higher than that observed for ACHE and, while in the latter case only the enol tautomer forms inclusion complexes with $\beta\text{-CD}$, in the case of ATLO both keto and enol tautomers form inclusion complexes with $\beta\text{-CD}$. The complexed enol is unreactive for both substrates in nitrosation, by contrast, the complexed enol of ATLO undergoes also tautomerization.

Acknowledgements

Financial support from the Dirección General de Investigación (Ministerio de Ciencia y Tecnología) of Spain (Project BQU2000-0239-C02-01) is gratefully acknowledged.

References

1. E. Iglesias: *Curr. Org. Chem.* **8**(1), 1–24 (2004).
2. T.W. Bentley and P. von R. Schleyer: *Adv. Phys. Org. Chem.* **14**, 1–67 (1977).
3. C. Reichardt: *Solvent and Solvent Effect in Organic Chemistry*, 2nd edn, Chap.5, VCH Verlagsgesellschaft, Weinheim (1988).
4. E.M. Kosower: *Physical Organic Chemistry*, Wiley, London (1968).
5. C. Reichardt: *Solvent and Solvent Effect in Organic Chemistry*, 2nd edn, Chap.2, VCH Verlagsgesellschaft, Weinheim (1988).
6. E.J. Fendler and J.H. Fendler: *Catalysis in Micellar and Macromolecular Systems*, Academic Press, New York (1975).
7. C.A. Bunton and G. Savelli: *Adv. Phys. Org. Chem.* **22**, 231 (1986).
8. G. Savelli, R. Germani and L. Brinchi: In J. Texter (ed.), *Reaction and Synthesis in Surfactant Systems*, Surfactant Science Series, Vol.100, Marcel Dekker, New York (2001) pp. 175–246.
9. J. Szejtli: *Cyclodextrin Technology*, Kluwer, Dordrecht, The Netherlands (1988).
10. J. Szejtli: *Chem. Rev.* **98**, 1743 (1998).
11. M. Cortijo, J. Llor and J.M. Sánchez-Ruiz: *J. Biol. Chem.* **263**, 17960 (1988).
12. J. Llor, J.M. Sánchez-Ruiz and M. Cortijo: *J. Chem. Soc., Perkin Trans. II*, 951 (1988).
13. E. Iglesias and D.L.H. Williams: *J. Chem. Soc. Perkin Trans. II*, 1035(1998) and references therein.
14. (a) J. Toullec: In Z. Rappoport (ed.), *The Chemistry of Enols*, J. Wiley & Sons, Chichester, England (1990) pp. 323–398; (b) J. Toullec: *Adv. Phys. Org. Chem.* **18**, 1 (1982).
15. S. Forsén and M. Nilsson: In J. Zabicky (ed.), *The Chemistry of the Carbonyl Group*, Vol. 2, Interscience Publishers, John Wiley & Sons (1970) p. 200.
16. (a) E. Iglesias: *J. Phys. Chem.* **100**, 12592 (1996); (b) E. Iglesias: *J. Chem. Soc. Perkin Trans. 2*, 431 (1997).
17. (a) E. Iglesias, V. Ojea-Cao, L. García-Río, and J.R. Leis, *J. Org. Chem.* **64**(11), 3954 (1999); (b) E. Iglesias: *J. Org. Chem.* **65**(20), 6583 (2000).
18. (a) E. Iglesias: *J. Org. Chem.* **68**(7), 2680 (2000); (b) E. Iglesias: *J. Org. Chem.* **68**(7), 2689 (2003).
19. (a) E. Iglesias: *Langmuir*, **16**(22), 8438 (2000); (b) E. Iglesias: *New J. Chem.* **26**, 1352 (2002).
20. J.E. Anderson: *J. Phys. Chem.* **95**, 7062 (1991).
21. R.I. Geld, L.M. Schwartz, M. Radeos, R.B. Edmonds and D.A. Laufer: *J. Am. Chem. Soc.* **104**(23), 6283 (1982).
22. M.V. Rekharsky and Y. Inoue: *Chem. Rev.* **98**, 1875 (1998).